Excimer Formation of Dimethyl 2,6-Naphthalene Dicarboxylate Embedded in a Poly(methyl methacrylate) Matrix

C. Spies* and R. Gehrke

Hamburger Synchrotronstrahlungslabor HASYLAB at Deutsches Elektronensynchrotron DESY, Notkestr. 85, 22603 Hamburg, Germany

Received: November 14, 2001

Dimethyl 2,6-naphthalene dicarboxylate (DMN) was embedded in a poly(methyl methacrylate) (PMMA) matrix. According to the molecular weight of the repeating unit of PMMA different samples containing 0.02 up to 8 mol % DMN have been prepared. Starting from 1 mol % DMN content, excimer formation is observed. From time-resolved fluorescence experiments the fluorescence lifetime of the monomer was derived to be 15 ns and the excimer lifetime amounts to 30 ns. It was shown that Förster excitation energy transfer takes place among the DMN monomers and the Förster radius of the monomer was determined by time-resolved fluorescence depolarization experiments to be 23 ± 3 Å. Excitation energy transfer is assumed to be the dominant process for the excimer formation. Using a model of three-dimensional transport among DMN donors until an excimer trap is reached, dimensionless trap concentrations of 0.005 and 0.014 were derived for the samples with 1 and 2 mol % DMN, respectively. For larger DMN concentration the excitation energy transfer between DMN molecules becomes anisotropic.

Introduction

Time-resolved fluorescence and fluorescence depolarization experiments are used to obtain detailed information about excimer formation in the solid state. In this paper the mechanism of excimer formation of dimethyl 2,6-naphthalene dicarboxylate (DMN) embedded in a poly(methyl methacrylate) (PMMA) matrix will be discussed. DMN was chosen as it serves as a model compound for the fluorescent unit of the polymer poly(ethylene-2,6-naphthalene dicarboxylate) (PEN).[1−3] Aromatic polyesters such as PEN and poly(ethyleneterephthalate) (PET) show dominant excimer emission if the monomeric unit is excited[1,4,5] and additionally ground-state stable dimer emission was observed.[6] Excimers and ground-state stable dimers are distinguished because an excimer is formed by interaction of an excited monomer with a second monomer in the electronic ground state.[7] In contrast, ground-state stable dimers are excited as an ensemble of two monomers.[6] In PET, ground-state stable dimer excitation is red shifted compared to the excitation of the monomeric unit.[6] Jones et al.[8] reported on excimer and ground-state stable dimer emission in PEN-*co*-PET copolyesters. The lifetime of the PEN monomer unit which is similar to that of DMN was found to be 12 ns in the PET matrix. They suggest that dimers and excimers formed in PEN have the same fluorescence lifetime of about 26.5 ns.[8] In contrast, analysis of the PET fluorescence shows that the decay is much faster if ground-state stable dimers are excited compared to emission of excimers formed by exciting the monomeric units.[9,10] Additionally in PET the emission of ground-state stable dimers is not single exponential.[9,10] In this paper we will focus on excimer emission.

The basic investigations on excimer formations in solutions have been performed by Döller and Förster[11] and Birks et al.[12] on pyrene solutions. They found that excimer formation in solution is a diffusion-controlled process, therefore the encounter of an excited molecule and a second one in the ground state is the rate-determining step. For the excimer formation of DMN solved in chloroform and HFIP the rate of excimer formation was found to be only less than 1 order of magnitude smaller than the rate of diffusion calculated for the pure solvent k_{diff}.[3] As k_{diff} was calculated for the solvent−solvent interaction and not for the solute−solvent interaction it was concluded that also for DMN in solutions the excimer formation is a diffusion-controlled process.[3] In the solid state the fluorescent sites are localized at certain positions. We assume excimers to be sandwich-like formations of two aromatic rings. As a distribution of distances is realized in the solid state some aromats might be close enough to each other to transform to excimers if one of the partners is excited. Thus, if the rate of excimer formation is assumed to be very fast, as observed in solution, time-resolved fluorescence experiments will provide detailed information about the mechanism of excimer formation. If the excitation energy is localized on the initially excited monomers, i.e., the monomers that were excited by the excitation light pulse, a site able to build an excimer will immediately transfer to this. The time-resolved fluorescence curve will instantaneously decay and excimer formation will then be indistinguishable from direct excitation. As in our case a time-delayed maximum is observed in the excimer emission, a delayed mechanism of excimer formation must exist. We will show that Förster excitation energy transfer[13,14] takes place in the samples investigated in this work and that this excitation energy transfer is the main process leading to excimer formation.

Experimental Section

Sample Preparation. PMMA films have been prepared containing 0.02, 0.1, 1, 2, 4, and 8 mol % DMN. DMN purchased from Aldrich was purified by sublimation at 160 °C and 2 mbar. PMMA was purchased from Degussa. The content of DMN was calculated in mol % with respect to the molecular

* Author to whom correspondence should be addressed. E-mail: spies@desy.de.

10.1021/jp014178z CCC: $22.00
Published on Web 05/04/2002

weight of the repeating unit of PMMA. The calculated amounts of DMN and PMMA were dissolved in methylene chloride UVASOL from Merck. The methylene chloride was evaporated slowly and the substances were dried at 80 °C under vacuum for several hours. Amorphous films of about 200 μm thickness have been prepared by melt-pressing for 70 s at 280 °C and subsequent quenching in iced water.

Fluorescence Spectra and Time-Resolved Fluorescence Measurements. Fluorescence spectra were measured with an Aminco SPF-500 spectrofluorometer in reflection geometry. Time-resolved fluorescence measurements were performed at the beamline VISUV (VISible and UV) at the Hamburger Synchrotronstrahlungslabor HASYLAB at Deutsches Elektronensynchrotron DESY. The storage ring DORIS is used as a pulsed light source. DORIS delivers light pulses of about 150 ps (fwhm) with 2 or 5 MHz repetition rate depending on the operation mode. The excitation light was monochromatized by a grating monochromator (Jobin Yvon type H10UV, bandwidth 16 nm) and the luminescence light passed through a second monochromator (Jobin Yvon type H320, bandwidth 4 nm). For single photon counting detection a microchannel plate photomultiplier type R3809U-50 from Hamamatsu was used. The instrument response function was observed by scattering at milk (fwhm about 300 ps). The polymer films were measured in transmission geometry with fluorescence detection perpendicular to the excitation direction. All measurements were carried out at 288 K. Acquisition times were varied from about one minute to about 1 h to observe fluorescence curves with at least 30000 counts in the maximum channel. The time interval between adjacent data points was 196 ps.

Time-Resolved Fluorescence Depolarization. To obtain vertically polarized excitation light, a Glan-Taylor prism purchased from Melles Griot was mounted after the primary monochromator. The PMMA films were measured in transmission geometry. The fluorescence light was recorded perpendicular to the direction of the excitation light after passing through a Glan-Thomson prism and a band-pass filter (bandwidth 40 nm). The emission anisotropy $r(t)$ was calculated using the equation

$$r(t) = (I(t)_{vv} - gI(t)_{vh})/(I(t)_{vv} + 2gI(t)_{vh}) \qquad (1)$$

The first index v indicates the vertically polarized primary beam. The second index v or h characterizes the polarization direction of the fluorescence light, i.e., the analyzer orientation. The analyzer orientation was changed every 100 s between horizontal and vertical to realize identical excitation conditions for both recorded fluorescence decay curves. The fluorescence intensity was corrected for detector dead time. Fluorescence decay curves with at least 50000 up to about 200000 counts in the maximum channel were recorded. The factor g was introduced in eq 1 to correct for the dependence of the optics on the polarization direction. It was determined by exciting the sample with horizontally polarized light and measuring the fluorescence in both perpendicular directions, i.e., analyzer vertically and horizontally oriented. In this case both recorded fluorescence decay curves should be identical. To correct for differences in the observed intensities, the factor g was calculated by the equation

$$g = I_{hv}/I_{hh} \qquad (2)$$

where I is the integral intensity of the measured time-resolved fluorescence curves determined by summing up over all data points. Additionally, all curves were initially background corrected by subtracting a constant value observed in the curve region of pure scattering.

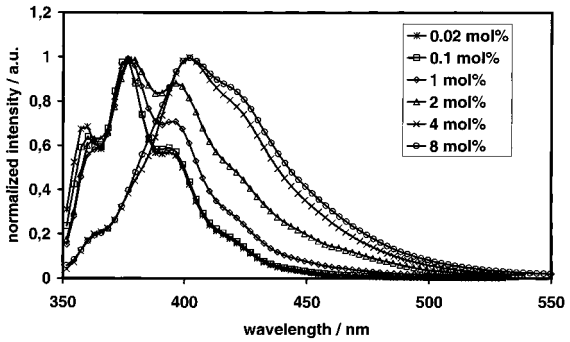

Figure 1. Fluorescence spectra of DMN in PMMA excited at 340 nm. The DMN content was varied from 0.02 to 8 mol %. The spectra are normalized to maximum intensity.

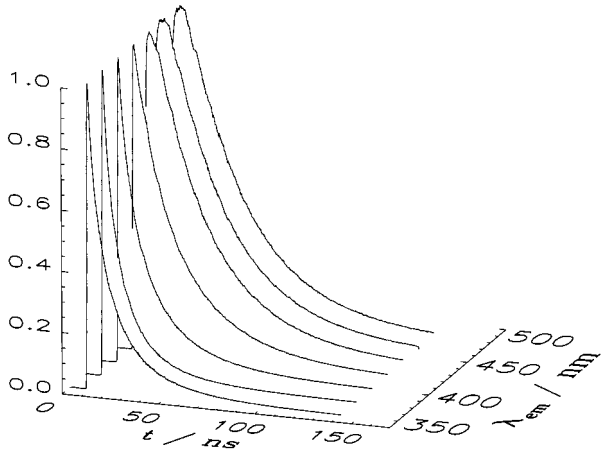

Figure 2. Time-resolved fluorescence decay curves of the sample containing 8 mol % DMN. The excitation wavelength was 340 nm and the emission wavelength was varied from 360 to 480 nm in 20 nm steps. The curves are normalized to maximum intensity.

Results and Discussion

PMMA films have been prepared containing 0.02, 0.1, 1, 2, 4, and 8 mol % DMN. Figure 1 shows the fluorescence spectra of the samples excited at 340 nm. This wavelength lies in the range of the lowest energy absorption band of DMN. Starting from 1 mol % DMN increasing emission intensity in the longer wavelength range is observed with increasing DMN concentration. This change of the fluorescence spectra indicates that excimer formation takes place at higher concentrations. A similar change of the fluorescence spectra was observed by Chen et al.[1] who investigated the fluorescence of DMN in chloroform solutions. To obtain more information about the mechanism of excimer formation in the solid-state time-resolved fluorescence decay curves of all samples have been measured. Figure 2 shows the fluorescence decay curves of the sample with 8 mol % DMN. It was excited at 340 nm and the emission was monitored from 360 to 480 nm in 20 nm steps. With increasing emission wavelength a broadening of the decay curves is observed and a delayed maximum appears. The delayed maximum shows that a delayed mechanism of excimer formation exists, i.e., a mechanism where excimers are not excited directly by the excitation light pulse. We assume that excimer-forming conformations are already realized during sample preparation. Excimers are formed in sandwich-like conformations of two adjacent aromatic rings.[2,7] Since a distribution of distances exists between the DMN species some of the DMN molecules could

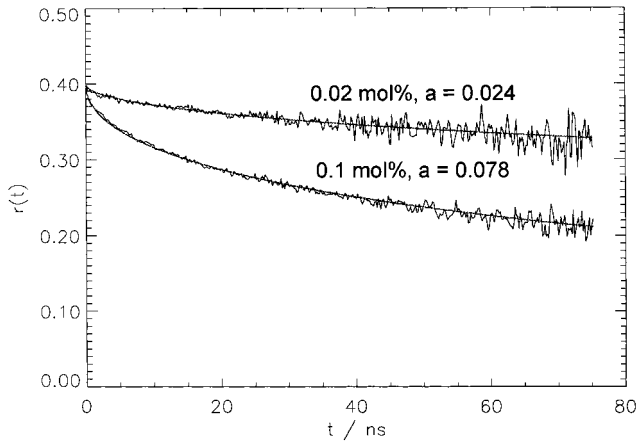

Figure 3. Comparison of the measured and calculated emission anisotropy $r(t)$ for the samples with 0.02 and 0.1 mol % DMN content. The value a is determined according to eq 7.

be close enough to each other to form sites which transfer to excimers if one the DMN partners is excited. In solutions, excimer formation is a diffusion-controlled process.[3,11,12] Since the rate constant of diffusion in solution is in the order of 10^{10} L mol^{-1} s^{-1} the rate of excimer formation is even larger. If we assume that excimer formation in the solid state also takes place on a comparably fast time scale, i.e., in the range of picoseconds then if one of the excimer forming partners is excited by the excitation light pulse on our observation time-scale we would not observe a delayed maximum in the decay curves. Since a delayed maximum is observed we suggest that it is caused by excitation energy transfer from DMN monomers to an excimer trap. For concentrations above 0.1 mol %, DMN excimer formation is observed. The excimers are assumed to act as traps for the excitation energy of the monomeric donors. To proof that excitation energy transfer takes place in the investigated samples we will first describe the observations made on the samples with low DMN content, where no excimer formation was found.

The excitation energy transfer in the absence of traps, i.e., only between so-called donor molecules, does not influence the fluorescence decay curve $I(t)$ but is observable in time-resolved fluorescence depolarization experiments.[15,16] The emission anisotropy $r(t)$ obtained for the samples with 0.02 and 0.1 mol % DMN is shown in Figure 3. It was calculated with eq 1 as described in the Experimental Section. The factor g was determined to be 0.98 for 0.02 mol % DMN and 1.01 for 0.1 mol %. It was proof that the excitation light pulse profile can be taken as a δ-function, therefore no deconvolution of the pulse and the decay curves was made. The representation of the $r(t)$ curves starts at time t that corresponds to the maximum of the excitation pulse profile.

A theoretical treatment of the loss of anisotropy in an isotropic donor−donor transfer system is given by Baumann and Fayer.[16] The following assumptions were made: (i) the orientation of the molecules is frozen so that the only process which depolarizes the fluorescence is excitation energy transfer; (ii) the directions of the absorption and emission moments in a given molecule are parallel; (iii) if the excitation energy is transferred to an adjacent molecule it can only return to the initially excited molecule but cannot be transferred to further molecules. Under these assumptions the calculated anisotropy function for an isotropic three-dimensional distribution of molecules is

$$r(t) = \frac{2}{125} + \frac{48}{125} G^{s}(t) \tag{3}$$

where $G^{S}(t)$ is the probability of finding an initially excited molecule still excited at time t.[16] We assume a system with randomly disordered molecule positions and rigid molecules isotropically oriented in three dimensions, thus[16]

$$\ln G^{s}st(t) = -c \cdot 2^{-1/2} \cdot \left(\frac{3}{2}\right)^{1/2} \cdot \langle|\kappa|\rangle \cdot \sqrt{\pi} \cdot \left(\frac{t}{\tau}\right)^{1/2} \tag{4}$$

For static, three-dimensional isotropic distribution of angles between coupling dipoles the value of $<|\kappa|> = 0.6901$.[16] Therefore, eq 4 can be written as

$$\ln G^{s}(t) = -c \cdot 1.0593 \cdot \sqrt{\frac{t}{\tau}}, \tag{5}$$

with the dimensionless concentration

$$c = \rho \frac{4}{3} \pi R_0^3 \tag{6}$$

where R_0 is the Förster radius and ρ is the number density of the inspected molecules. The number density ρ was calculated with the density of pure PMMA of 1.2 g/cm^3. For 0.1 mol % DMN $\rho = 7.226 \times 10^{-6}$ Å^{-3}, thus the number density of pure PMMA was divided by 1000. In the case of 0.02 mol % DMN content $\rho = 1.445 \times 10^{-6}$ Å^{-3}. The fluorescence lifetime τ was obtained from fits to the time-resolved fluorescence decay curves. For 0.02 mol % DMN $\tau = 13.8$ ns and for 0.1 mol % DMN $\tau = 15.1$ ns were obtained. The value increases due to reabsorption effects. Reabsorption also leads to a decrease of the emission anisotropy but this effect was neglected.

Figure 3 shows a comparison of the anisotropy curves derived from the measurement of $I_{vv}(t)$ and $I_{vh}(t)$ for the 0.02 and 0.1 mol % DMN samples with the theoretical anisotropy curve given by

$$r(t) = \frac{2}{125} + \frac{48}{125} \cdot \exp(-a \cdot \sqrt{t}). \tag{7}$$

The constants given in eq 5 were combined in one scaling factor a. Thus,

$$\ln G^{s}(t) = -a \cdot \sqrt{t}. \tag{8}$$

For the sample with 0.02 mol % DMN the best agreement between the anisotropy obtained from the measurements and the theoretical one was obtained for $a = 0.024$. With the values of the constants given above a Förster radius of 24 Å was calculated. For the sample containing 0.1 mol % DMN one obtains $a = 0.078$, leading to a Förster radius of 21 Å. Thus, for DMN in PMMA we obtained a Förster radius of 23 ± 3 Å. The main contribution to the error comes from the determination of the number density ρ.

Next the results from those samples will be interpreted where excimer formation is observed. Figure 4 shows the fluorescence decay curves of the samples containing 0.1 mol % and more DMN, excited at 340 nm and the emission monitored at 380 nm. It is known from the fluorescence spectra that no excimer formation is observed at 0.1 mol % DMN concentration. In accordance to this, a single exponential decay curve is observed represented in Figure 4 by the dashed line. This single exponential decay curve was measured at all emission wavelengths and a fluorescence lifetime of the monomer of about 15 ns was calculated. With increasing DMN concentration an increasing deviation from a single exponential is visible. Additional decay time components with short decay times arise. Also fluorescence arising from species with longer decay times

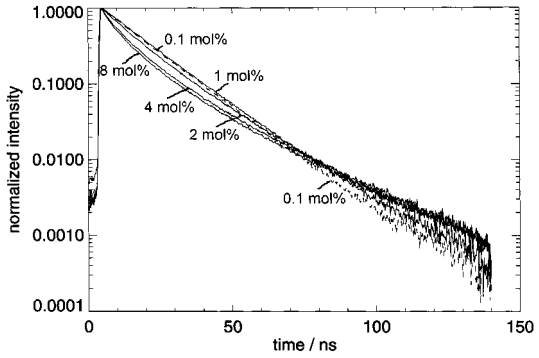

Figure 4. Time-resolved fluorescence decay curves of the samples with 0.1 (dashed line) to 8 mol % DMN. All samples were excited at $\lambda_{ex} = 340$ nm and the emission was monitored at $\lambda_{em} = 380$ nm.

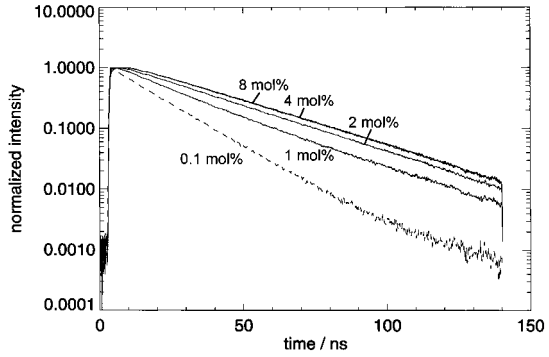

Figure 5. Time-resolved fluorescence decay curves of the samples with 0.1 (dashed line) to 8 mol % DMN. All samples were excited at $\lambda_{ex} = 340$ nm and the emission was monitored at $\lambda_{em} = 480$ nm, except for the sample with 0.1 mol % DMN which was monitored at $\lambda_{em} = 460$ nm for intensity reasons.

than the 15 ns of the pure monomer fluorescence is observed. Species with longer decay time are also visible at 360 nm emission wavelength but with slightly larger intensity than observed at 380 nm. We attribute this longer decay time to excimer emission. As the ratio of excimer to monomer emission is slightly larger at 360 nm compared to 380 nm we conclude that a back-reaction from an excimer to an excited monomer is negligible in the solid state. This means that the monomer emission is weaker at 360 compared to 380 nm, thus, a small amount of overlaid excimer emission could be more pronounced at 360 than at 380 nm. We assume the excimers starting to emit around 360 nm. If, on the other hand, the long decay time component would be generated by a back-reaction from an excimer to an excited monomer one should observe a constant amount of the long decay time component in the range of pure monomer emission and an increasing amount with increasing emission wavelength.[3] All recorded decay curves in the emission range from 360 to 480 nm for all the samples with DMN contents of 1 mol % and more show a decay time component of 30 ± 2 ns, as known from fits to the measured curves with sums of exponential functions. We conclude that the 30 ns decay time component can be attributed to the excimer lifetime. If a distribution of excimer lifetimes exists, for instance due to different distances of the two aromats, they are not distinguishable in our experiment. As an example, the decay curves measured at the emission wavelength of 480 nm are shown in Figure 5. Additionally the decay time components and the corresponding amplitudes of the best fits of three exponentials to the decay curves shown in Figure 5 are given in Table 1.

The delayed maximum is more pronounced for the samples with larger DMN content. As known from the spectra shown in Figure 1 the portion of excimers is larger in the samples with large DMN concentrations. Taking the model excitation energy transfer from monomer donors to excimer traps into account the time delay should be larger for low trap concentrations. Thus, we conclude that at 480 nm a small amount of monomer emission is still overlaid. To combine measured decay curves with theoretical ones it is necessary to know the decay behavior of the pure monomer or the pure excimer as the ratio of monomer to excimer emission is unknown. To obtain the pure monomer emission curves a weighted subtraction was performed. For this purpose, the decay curves measured at 480 and 380 nm emission wavelengths have been normalized to identical intensity in the time range about 130 ns. At this time the monomer emission has vanished. Then the normalized curve measured at 480 nm was subtracted from the normalized curve measured at 380 nm. The difference curves are represented in Figure 6. The curves obtained for the samples with 1 and 2 mol % DMN are nearly single exponential. For the curves with 4 and 8 mol % DMN a clear deviation from the single-exponential behavior is visible on the short time scale.

To obtain the trap concentration, a comparison between a theoretical study of trapping of excitation energy in a donor ensemble with only a small number of traps and the monomer decay curves represented in Figure 6 was carried out. A theoretical treatment of this trapping phenomenon is given by Huber[17,18] and Loring et al.[19] They calculated the Laplace transform $\hat{G}^D(0,\epsilon)$ of $G^D(t)$, which is the probability that the excitation is in the donor ensemble assuming infinite lifetimes.

$$\hat{G}^D(0,\epsilon) = \left\{ \epsilon + \frac{\pi}{2} C_T \left[\frac{1}{\tau \hat{G}^S(\epsilon)} \right]^{1/2} \right\}^{-1} \tag{9}$$

with

$$G^S(t) = \exp\left[-\left(\frac{\pi}{2\tau} \right)^{1/2} C_D t^{1/2} \right] \tag{10}$$

where C_D and C_T represent the dimensionless donor and trap concentration, respectively, and τ is the donor lifetime in the absence of traps. Equation 9 should be valid if the trap concentration is low compared to the donor concentration. It was derived for the energy transport in solutions. In the case of direct trapping it is known that only a scaling factor is required to consider a rigid distribution of absorption and emission moments instead of the fast diffusion limit.[16] Therefore, we assume that eq 9 should be a good approximation for the solid-state transport, too.

Figure 7 shows a comparison of the difference curve for 1 mol % DMN, i.e., the pure monomer decay and the calculated decay

$$I(t) = G^D(t) \exp(-t/\tau) \tag{11}$$

Equation 10 was Laplace transformed analytically and inserted into equation 9. $G^D(t)$ was obtained by a numerical Laplace inversion using the Stehfest algorithm.[20] The dimensionless donor concentration was calculated with eq 6 assuming a Förster radius of 23 Å and a number density $\rho = 7.226 \times 10^{-5}$ Å^{-3}, calculated from the density of pure PMMA. The value of C_D is 3.7. The donor lifetime τ was taken to be 15 ns. The best agreement between experimental and theoretical curve was obtained for a dimensionless trap concentration $C_T = 0.005$. Additionally, for the sake of comparison the theoretical undisturbed monomer decay $\exp(-t/\tau)$ with $\tau = 15$ ns is represented in Figure 7.

TABLE 1: Decay Times and Corresponding Amplitudes Obtained from Fits with a Sum of Three Exponential Functions on the Decay Curves Represented in Figure 5 ($\lambda_{ex} = 340 \pm 8$ nm, $\lambda_{em} = 480 \pm 2$ nm)

DMN content/ mol %	τ_1/ ns	A_1/ %	τ_2/ ns	A_2/ %	τ_3/ ns	A_3/ %	χ^2	counts at maximum
1	3.8 ± 0.2	-13 ± 1	14.6 ± 0.4	41 ± 1	28.8 ± 0.2	46 ± 1	1.64	35000
2	3.6 ± 0.1	-18 ± 1	15.3 ± 0.9	8 ± 1	29.6 ± 0.1	74 ± 1	1.50	44000
4	3.0 ± 0.1	-20 ± 1	9.9 ± 0.8	-8 ± 1	30.1 ± 0.1	72 ± 0.3	1.84	51000
8	2.4 ± 0.2	-19 ± 1	7.1 ± 0.6	-11 ± 1	29.9 ± 0.1	71 ± 0.2	1.28	33000

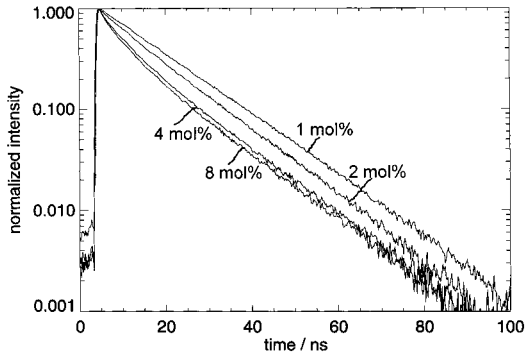

Figure 6. Decay curves representing the pure monomer decay of the samples with 1 to 8 mol % DMN content. They were obtained by subtraction of the normalized curves measured at $\lambda_{em} = 480$ nm from $\lambda_{em} = 380$ nm ($\lambda_{ex} = 340$ nm).

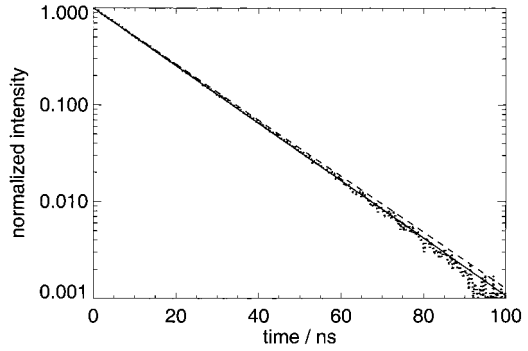

Figure 7. Comparison of difference curve of 1 mol % DMN, i.e., pure monomer decay (dots), and the theoretical decay given by eq 11 (solid line). Additionally, the exponential decay $\exp(-t/\tau)$ with $\tau =$ 15 ns is shown (dashed line).

For the difference curve of 2 mol % DMN in PMMA the donor concentration is 7.4 and a good agreement between measured and calculated curve was obtained for a trap concentration of $C_T = 0.014$. For higher donor concentrations eq 11 fails. For these large values of C_D, i.e., 14.7 and 29.5 for 4 and 8 mol % for all reasonable values of C_T the decay function is too close to a single exponential. We were not able to describe the non exponential behavior at the short time range for these large donor concentrations. We also tried eq 54 given by Loring et al.[19] which is also valid for large trap concentrations but again the observed behavior was not reached. As known from calculations concerning the transport phenomenon on periodic lattices, a deviation from the single-exponential becomes more pronounced if the transport is reduced in dimensionality, i.e., if it is less than three-dimensional.[21,22] We assume that for the samples with large concentrations the transport becomes anisotropic. The mean distance of DMN molecules is in the range of the molecule dimensions now, which might case an anisotropy. To find evidence for this wide-angle X-ray scattering (WAXS), measurements have been performed. These results will be applied to the calculation of the transport behavior of the samples with the high concentrations and will be the topic of another paper.

Conclusions

We conclude that conformations which can lead to excimers are already realized during sample preparation. According to the fluorescence spectra a maximum value of the trap density seems to be attainable and it is not achieved at 8 mol % DMN content. As a delayed maximum is observed in the time-resolved fluorescence measurements, when excimer emission is dominant, the process of excimer formation is time delayed. We suggest that Förster excitation energy transfer among the DMN monomers until an excimer trap is reached is the main process of excimer formation. In the PMMA matrix the excimers start to emit around 360 nm and act as real traps for the monomer excitation energy, i.e., a back-reaction from an excited excimer to an excited monomer is negligible in the solid state. Furthermore we assume that the excimer lifetime is 30 ns. If a distribution of excimer lifetimes exists, e.g., due to different distances, it is not detectable in our experiment.

Acknowledgment. We thank Prof. Kricheldorf for giving the opportunity of sample preparation in his laboratory. One of the authors thanks the Deutsche Forschungsgemeinschaft (DFG) for financial support under Contract Sp 574/1-3 and 1-4.

References and Notes

(1) Chen, S.; Bai, F.; Quian, R. *Sci. Sin. (Engl. Ed.)* **1981**, *24*, 639.
(2) Spies, C.; Gehrke, R. *Macromolecules* **1997**, *30*, 1701.
(3) Spies, C.; Gehrke, R. *J. Lumin.* **1999**, *82*, 333.
(4) Cao, T.; Magonov, S. N.; Quian, R. *Polym. Commun.* **1988**, *29*, 43.
(5) Spies, C.; Gehrke, R. *Macromolecules* **1999**, *32*, 8383.
(6) Hennecke, M.; Fuhrmann, J. *Makromol. Chem., Macromol. Symp.* **1986**, *5*, 181.
(7) Renamayor, C. S.; Gomez-Anton, M. R.; Calafate, B.; Mano, E. B.; Radic, D.; Gargallo, L.; Freire, J. J.; Pierola, I. F. *Macromolecules* **1991**, *24*, 3328.
(8) Jones, A. S.; Todd, J. D.; Wilson, B. E.; Duhamel, J. *Macromolecules* **1999**, *32*, 2956.
(9) Hemker, D. J.; Frank, C. W.; Thomas, J. W. *Polymer* **1988**, *29*, 437.
(10) Hennecke, M.; Kud, A.; Kurz, K.; Fuhrmann, J. *Colloid Polym. Sci.* **1987**, *265*, 674.
(11) Döller, E.; Förster, T. *Z. Phys. Chem. Neue Folge* **1962**, *34*, 132.
(12) Birks, J. B.; Dyson, D. J.; Munro, I. H. *Prog. R. Soc. A* **1963**, *275*, 575.
(13) Förster, T. *Z. Naturforschung* **1949**, *4a*, 321.
(14) Förster, T. *Discuss. Faraday Soc.* **1959**, *27*, 7.
(15) Gochanour, C. R.; Fayer, M. D. *J. Phys. Chem.* **1981**, *85*, 1989.
(16) Baumann, J.; Fayer, M. D. *J. Chem. Phys.* **1986**, *85*, 4087.
(17) Huber, D. L. *Phys. Rev. B* **1979**, *20*, 2307.
(18) Huber, D. L. *Phys. Rev. B* **1979**, *20*, 5333.
(19) Loring, R. F.; Andersen, H. C.; Fayer, M. D. *J. Chem. Phys.* **1982**, *76*, 2015.
(20) Stehfest, H. *Commun. ACM* **1970**, *13*, 47; **1970**, *13*, 624.
(21) Zumofen, G.; Blumen, A. *Chem. Phys. Lett.* **1982**, *88*, 63.
(22) Movaghar, B.; Sauer, G. W.; Würtz, D. *J. Stat. Phys.* **1982**, *27*, 473.